JOURNAL OF THE TENNESSEE ACADEMY OF SCIENCE
VOLUME 36, NUMBER 2, APRIL, 1961

THE NEUTRON AS A PROBE OF NUCLEAR MATTER

J. L. FOWLER
Oak Ridge National Laboratory
Oak Ridge, Tennessee

Since its discovery in 1932, the neutron has served as a powerful probe of the structure of nuclei. Its lack of charge allows even a very low energy neutron to approach the nucleus without suffering the intense Coulomb repulsion which is experienced by other nuclear particles such as a proton or an alpha particle. This lack of Coulomb repulsion greatly simplifies the analysis of neutron data. An approximate analysis is simplified even further in the case of neutrons of relatively high energy (>10 Mev); at relatively low energy (~1 Mev) a more exact analysis is feasible.

At high energy the De Broglie wavelength of the neutron, λ, divided by 2π, $\lambda\!\!\!^{-}$, is somewhat smaller than the radius of heavy nuclei ($\sim 10^{-12}$ cm). For 14-Mev neutrons

$$\lambda\!\!\!^{-} = h/(2\pi\sqrt{2mE}) = 1.23 \times 10^{-13} \text{ cm} ,$$

where h is Planck's constant, m is the mass in grams of a neutron, and E is its energy in ergs. Under these conditions the scattering and absorption of neutrons by nuclei appear somewhat similar to the scattering and absorption of light in simple problems of optics. The ease of an approximate interpretation resulting from the use of optical analogy enabled physicists relatively early in the history of nuclear science to arrive at an estimate of the size and density of nuclei from neutron total cross section measurements (Sherr, 1945).

In general, a neutron cross section is defined as the probability of a neutron producing an effect of a given type as follows:

$$\sigma = \frac{\text{number of events per unit time per nucleus}}{\text{number of neutrons per unit area per unit time}} . \qquad (1)$$

If the event is the deflection or removal of a neutron from a beam, then the cross section is called the total cross section, σ_T. One can also think of the total cross section of a nucleus for a neutron as the effective projected area of the nucleus, σ_T, such that if the neutron hits within this area it will be removed from the beam. Total neutron cross sections are found experimentally by a simple measurement of the attenuation of a neutron beam by the samples being investigated (Marion and Fowler, 1960–61).

Since 14-Mev neutrons are readily available from the $T(d,n)He^4$ reaction (Marion and Fowler, 1960–61), accurate total cross sections have been measured for a number of nuclei at this energy (Hughes and Schwartz, 1958). By use of high-energy cyclotrons, neutrons of relatively high energy (~100 Mev) can be produced for total cross section measurements. Results of such measurements are collected in a set of curves in the publication "Neutron Cross Sections" (Hughes and Schwartz, 1958). Historically, the high-energy cross section measurements have been interpreted in terms of an optical model. Although a very simple analysis based on this model gives only a qualitative fit to the data, a more sophisticated handling of the model permits a rather good fit to the experimental information. The following qualitative arguments lead to the expression (Blatt and Weisskopf, 1952, p. 324)

$$\sigma_T = 2\pi(R^2) \quad , \tag{2}$$

which was used in the early interpretation of the data on total cross sections for neutrons of energy ~25 Mev (Sherr, 1945). The projected area of the nucleus of radius r, as seen by the neutron moving toward it, is given by

$$\pi(r + \lambda\!\!\!^{-})^2 = \pi R^2 \quad . \tag{3}$$

$\lambda\!\!\!^{-}$ shows up as the effective radius of the neutron. As an approximation, suppose the nucleus is black to neutrons; that is, suppose that every neutron which strikes the nucleus is absorbed out of the beam. In Fig. 1 (upper left-hand corner) the wave front associated with the incident neutron is represented by the series of vertical lines. πR^2 of this wave is removed by absorption of the nucleus. Because of diffraction effects, the nucleus does not cast a sharp shadow; but in a distance the order of $R^2/\lambda\!\!\!^{-}$, the wave will have been diffracted in such a way that behind the

nucleus the situation will be as shown in Fig. 1. One can estimate the probability of the neutron being scattered out of the beam by this diffraction phenomenon by means of the following qualitative considerations. Suppose at the position of the nucleus one considers neutrons emitted as if they came from the back of the disk of radius R with the same wavelength of the initial neutrons but 180° out of phase. Then immediately behind the nucleus the waves will cancel and one will find a region in space in which there is small probability of finding the neutron as indicated in Fig. 1. These out-of-phase neutrons will diverge from the initial direction in a distance R^2/λ, so that one will have a diffraction effect. The number of neutrons introduced

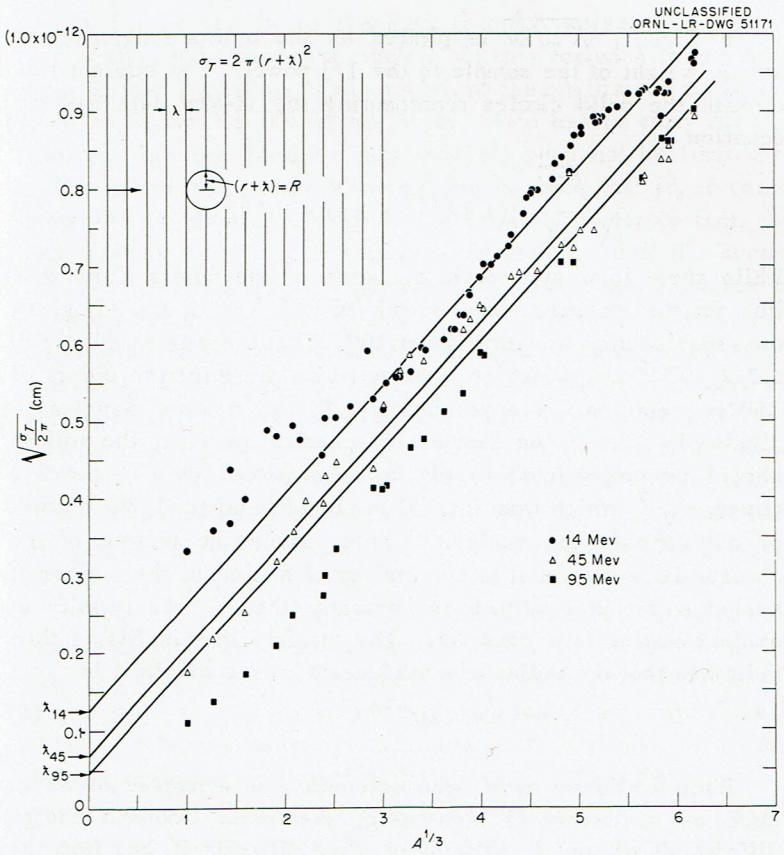

Fig. 1. Nuclear radii from fast neutron total cross sections.

with this shift in phase will be the same as the number removed from the beam by the black nucleus. This number is equal to πR^2 per nucleus. Therefore, in addition to the probability per nucleus of the neutrons being absorbed out of the beam πR^2, there is an equal probability πR^2 of the neutrons being diffracted out of the beam. The total cross section then, either for absorption or scattering, is given by Eq. (2). Thus if one divides the measured total cross section, σ_T, by 2π and takes the square root of the result, according to Eq. (2) one obtains the quantity

$$r + \lambda\!\!\!^{-} = \sqrt{\frac{\sigma_T}{2\pi}} \quad . \tag{4}$$

In Fig. 1, $\sqrt{\sigma_T/2\pi}$ is plotted as the ordinate against the atomic weight of the sample to the 1/3 power. The straight line through the solid circles representing the 14-Mev data has the equation

$$\sqrt{\frac{\sigma_T}{2\pi}} = (1.4A^{1/3} + 1.2) \times 10^{-13} \text{ cm} \quad . \tag{5}$$

While there is a systematic variation of the points about this line for the isotopes above aluminum ($A^{1/3} = 3$), Eq. (5) gives the cross section to within about 10%. The intercept at $A^{1/3} = 0$, 1.2×10^{-13} cm, which is interpreted as the effective radius of 14-Mev neutrons, is approximately $\lambda\!\!\!^{-}$, the neutron wavelength divided by 2π. If one assumes a spherical nucleus, the volume should be proportional to the cross sectional area to the 3/2 power, $\sigma_T^{3/2}$, which from Eq. (5) is proportional to A, the number of nucleons in the nucleus. Thus, since the volume of the nucleus is proportional to the number of nucleons, the number of nucleons per unit volume is constant; that is, the density of nuclear matter is a constant. The straight line in Fig. 1 then indicates that the radius of a nucleus of atomic weight A is

$$r = 1.4 \times 10^{-13} A^{1/3} \text{ cm} \quad . \tag{6}$$

Radii of nuclei have been determined in a number of ways, such as scattering of high-energy electrons, Coulomb energy differences of nuclei of the same A but different Z, and from the lifetime of heavy nuclei for alpha emission. All of these methods and many others (*Revs. Modern Phys.*, 1958) give approximately

the same results as those indicated by the neutron total cross section measurements as described above.

According to the simple analysis, the cross section at 45 and 95 Mev neutron energy should be given by the parallel lines shifted down by the differences in $\lambda\!\!\!^{-}$ for neutrons of 45 and 95 Mev from $\lambda\!\!\!^{-}$ for 14-Mev neutrons. As indicated by the data points, this is approximately true for the 45-Mev data, but for the 95-Mev data there is considerable deviation from the simple theory. While the elementary analysis is not really valid even for the 14- and the 45-Mev neutrons, at 95 Mev the model upon which the analysis is based breaks down even for medium-weight nuclei. At this energy the nucleus (particularly in the light- and medium-weight regions) becomes transparent to the neutrons.

In Fig. 1 the fit to the data is much worse for low-mass nuclei than it is for heavy nuclei. In this region $\lambda\!\!\!^{-}$ is not much smaller than the radius of the nuclei, so the qualitative arguments used to derive Eq. (2) do not apply. One has to carry out the analysis in more detail. This analysis need not be limited to cases in which the neutron wavelength is short, that is, to cases in which the neutron energy is high. As a matter of fact, the experimental data is susceptible to interpretation if the energy is low, even negative. Information on the bound states of neutrons in nuclei (the negative energy states) is extremely important for the study of nuclear structure. Experiments on the scattering and binding of neutrons by O^{16} are particularly revealing. O^{16} is to nuclear spectroscopy as a noble gas is to atomic spectroscopy. The eight protons and eight neutrons in O^{16} form tightly bound closed shells, so that the O^{16} nucleus behaves toward a neutron much as if it were an average potential of interaction somewhat similar to the situation in atomic spectroscopy for an atom just above the closed atomic shells.

There are, however, significant differences between the details of nuclear and atomic spectroscopy. In the case of atoms the Coulomb forces between particles are well known, whereas in the case of nuclei, the internucleon forces are more complicated and less completely understood. In the case of nuclei, the magnitude of the coupling between the spin of the nucleon and its orbital motion in the field of the nucleus is very much larger than is the case for the electrons in atoms, and this coupling is of opposite sign in the two cases. This spin-orbit coupling, which in the case of atoms results in a small splitting

of the energy levels, leads in nuclei to a different ordering in the filling of nuclear shells (Eisenbud and Wigner, 1958). In nuclear spectroscopy the system of labeling energy levels is slightly different from that customary in atomic spectroscopy. As an example, consider the ground state of a neutron bound to O^{16}, that is, the ground state of O^{17}. This state is designated as a $1d_{5/2}$ level. The number "1" signifies the number of zeros in the radial wave function of the neutron. This is different from the principal quantum number designation of atomic spectroscopy. The letter "*d*" gives the orbital angular momentum quantum number of this neutron; in the example $l = 2$. (*s*, *p*, *d*, *f*, *g*, etc., as in the case of atomic spectroscopy mean $l = 0, 1, 2, 3, 4$, etc.) The subscript 5/2 gives the total angular momentum quantum number of the state; in the example $l + 1/2 = 5/2$.

The observed energy-level diagram (Ajzenberg-Selove and Lauritsen, 1959) for states in O^{17} with even values of orbital angular momentum quantum numbers (l = even), that is, for states with even parity, is given in the upper left-hand corner of Fig. 3. The ground state as mentioned above is a $1d_{5/2}$ state; the first excited state at −3.27 Mev is a $2s_{1/2}$ state. Both of the $1s_{1/2}$ states are already filled in the O^{16} core. The six $1p$ states $2(2l + 1)$ are also occupied in O^{16}, so that the next available single-particle states for a neutron bound to an O^{16} core are the $2s$ states or the $1d$ states. The $1d_{3/2}$ state at +0.94 Mev is a virtual state, and shows up in neutron total cross section and scattering measurements.

One of the problems arising in nuclear spectroscopy is that of finding the average potential which will give the observed energy levels. As a first approximation, consider this potential for a neutron due to the O^{16} core as being a square well:

$$\begin{aligned} V(r) &= -V_0 \ , \qquad r < a \ , \\ V(r) &= 0 \ , \qquad\quad r > a \ . \end{aligned} \tag{7}$$

Here r is the radial distance of the neutron from the center of the O^{16} core. As will be seen, the requirement that $2s_{1/2}$ states be bound by −3.27 Mev limits the values of V_0 and a which need to be considered. For an s state, $l = 0$ and the Schrödinger wave equation

$$\nabla^2\psi + \frac{2m}{\hbar^2}(E - V)\psi = 0 \tag{8}$$

reduces to

$$\frac{d^2u(r)}{dr^2} + \frac{2m}{\hbar^2}(E - V)u(r) = 0 \quad . \tag{9}$$

m is the reduced mass of the neutron,

$$m = \frac{\text{mass of neutron} \times \text{mass of } O^{16}}{\text{mass of neutron} + \text{mass of } O^{16}} \quad ,$$

with the wave function $\psi = u/r$ depending only upon r. Inside the potential well the solution of Eq. (9) which is zero at the origin is

$$u_i^b = A^b \sin \frac{\sqrt{2m(-E_b + V_0)}}{\hbar} r \quad , \tag{10}$$

where A^b is a constant.

For the bound $2s_{1/2}$ state, E_b is 3.27 Mev. Outside of $r = a$, the solution of Eq. (9) which falls off with distance is

$$u_0^b = B^b \exp\left(-\frac{\sqrt{2mE_b}}{\hbar} r\right) \quad . \tag{11}$$

The solutions of Eq. (9) must join smoothly at $r = a$ as shown in Fig. 2. For any a, only one value of V_0 will lead to two zeros in u ($2s$ state) and allow the internal and external wave functions to match smoothly at $r = a$. In order to single out the values of a and V_0 which best describe the $2s$ state of O^{17}, additional experimental information is required. This can be supplied by neutron scattering from O^{16}.

For neutron scattering of s waves ($l = 0$), Eq. (9) holds also. In the scattering case, $E_{c.m.}$, the energy of the neutron in the center-of-mass system, is positive. It can be shown (Schiff, 1955) that the potential due to the nucleus has the effect on the external wave function, which describes the neutron, of shifting the phase by an angle $\delta_{s_{1/2}}$ (see Fig. 2). It is also shown that the total cross section for scattering s-wave neutrons is related to this phase shift by the equation

$$\sigma_T = 4\pi\lambda\!\!\!^{-2} \sin^2 \delta_{s_{1/2}} \quad . \tag{12}$$

The total cross section and the differential cross section of neutron scattering from O^{16} have been analyzed in terms of

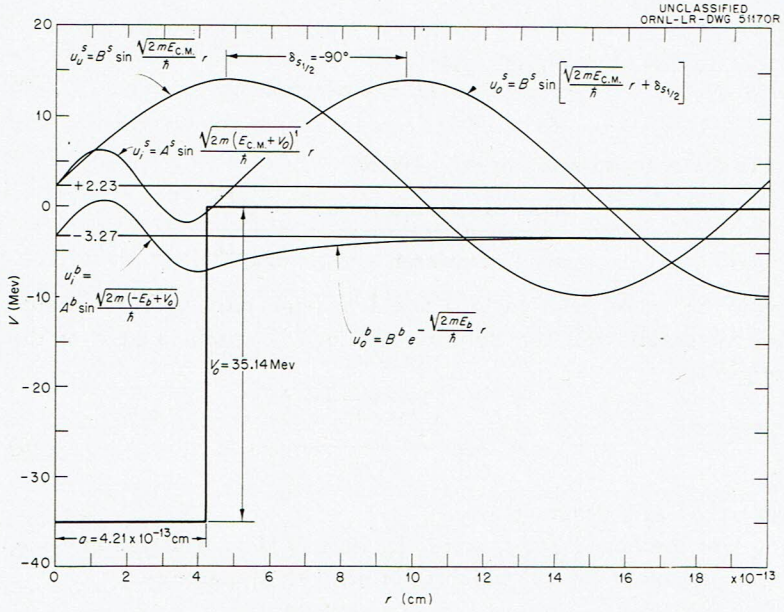

Fig. 2. Wave functions arising from a square well potential model for O^{17} 2*s* states.

the *s*-wave phase shifts $\delta_{s_{1/2}}$ and the phase shifts of higher angular momentum waves (Fowler and Cohn, 1958). At low enough energies the total cross section is entirely due to *s* waves, so that $\delta_{s_{1/2}}$ can be calculated from the total cross section data by use of Eq. (12). At 2.37 Mev in the laboratory system, there is a dip in the total cross section which is caused by interference between the continuous potential $\delta_{s_{1/2}}$ phase shift and a compound nucleus $s_{1/2}$ resonance. At such a resonance the phase shift goes through $+90°$ at the resonance energy. The shape of the dip means that the potential $\delta_{s_{1/2}}$ phase shift is $-90°$ at 2.37 Mev in order to just cancel the $+90°$ resonance phase shift at this energy. The unraveling of the phase shifts between low energies and 2.37 Mev is more complicated but is straightforward. Not only is the total cross section necessary, but also knowledge of the angular distribution of the scattered neutrons is needed. The points shown plotted in Fig. 3 give the results of the phase shift analysis based on this type of information (Fowler and Cohn, 1958).

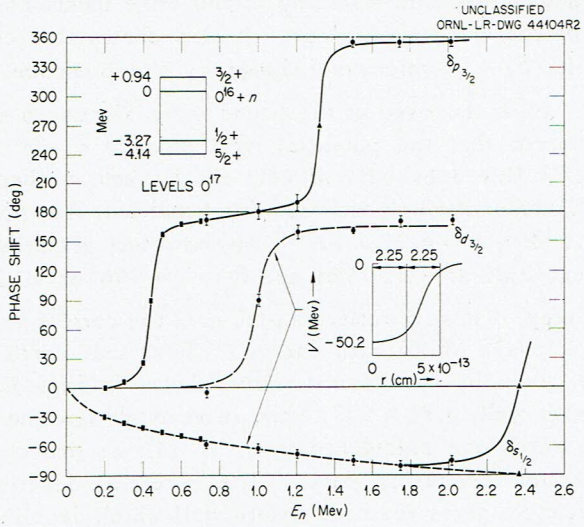

Fig. 3. Phase shifts for scattering of neutrons from O^{16}.

Since experimentally it is found that the potential s-wave phase shift is $-90°$ at a neutron laboratory energy of 2.37 Mev, the phenomenological nuclear potential which gives the $2s_{1/2}$ bound state at -3.27 Mev must also give this phase shift. This means that the potential well must alter the wavelength of a neutron at 2.23 Mev in the center-of-mass system (see Fig. 2), so that its phase relative to the wavelength of a free neutron is $-90°$. Mathematically, this condition is satisfied by requiring that the value of the wave function inside the nucleus, u_i^s, and its derivative, du_i^s/dr, match the corresponding quantities for the wave function u_0^s outside of the nucleus. For the square well,

$$u_i^s = A^s \sin \frac{\sqrt{2m(E_{c.m.} + V_0)}}{\hbar} r \ , \tag{13}$$

where

$$E_{c.m.} = \frac{\text{mass of neutron} \times \text{mass of } O^{16}}{\text{mass of neutron} + \text{mass of } O^{16}} E_{lab} \ , \tag{14}$$

$$u_0^s = B^s \sin \left(\frac{\sqrt{2mE_{c.m.}}}{\hbar} r + \delta_{s_{1/2}} \right) \tag{15}$$

Figure 2 shows how this matching of the wave functions at the boundary of the well takes place. It also shows the resulting phase shift, $\delta_{s_{1/2}}$, which is induced by the presence of the potential. As in the case of the bound state discussed earlier, the requirement that the potential well produce a $-90°$ phase shift at 2.23 Mev does not uniquely fix V_0 and a; there is a curve of V_0 versus a which satisfies this condition. The potential $V_0 = -35.1$ Mev, $a = 4.21 \times 10^{-13}$ cm, however, gives both the $2s_{1/2}$ bound state at -3.27 Mev and $\delta_{s_{1/2}} = -90°$ at $+2.23$ Mev neutron energy. These parameters also give the correct variation of the $s_{1/2}$ phase shifts with energy. These calculated phase shifts are given by the dashed curve shown in Fig. 3. The radius of this well, 4.21×10^{-13} cm, is in rough agreement with the value which one calculates from Eq. (4), as deduced from 14-Mev neutron scattering data. The potential described by these parameters gives the best square well which describes the single-particle properties of O^{17}.

If one pushes the analysis further, the square well approximation proves to be inadequate. This is not surprising; intuitively one suspects that there should be a diffuse boundary to the potential. In the calculation of the $1d$ states split by spin orbit coupling, the failure of the square well shows up. The well of radius 4.21×10^{-13} cm and of depth 35.1 Mev, which describes the s states, predicts too narrow a level for the $1d_{3/2}$ virtual state at 0.94 Mev and gives the binding of the $1d_{5/2}$ state much too low in energy.

A diffuse boundary to the potential can be introduced in a number of ways; a standard form, called the Woods-Saxon potential (Woods and Saxon, 1954) is represented by

$$V = \frac{-V_0}{1 + \exp\,(r - r_0)/\delta} \quad . \tag{16}$$

V_0 is the well depth and r_0 and δ are parameters of the dimension of length which can be adjusted to fit the data. The parameter δ, which defines the diffuseness of the boundary, can be selected to give the observed width of the $1d_{3/2}$ state. Then by the method illustrated in the discussion of the square well, V_0 and r_0 are determined by fitting the $2s_{1/2}$ state and the $s_{1/2}$ phase shifts. The $1d$ states require a spin orbit term in the potential.

This is usually taken in the Thomas form (Thomas, 1926; Inglis, 1936):

$$V_{s.o.} = \frac{-\gamma\hbar^2}{2m^2c^2}\,\frac{1}{r}\,\frac{\partial V}{\partial r}\left(\frac{\mathbf{l}\cdot\mathbf{s}}{\hbar^2}\right) . \qquad (17)$$

Here γ is an adjustable constant, c is the velocity of light, and $\mathbf{l}\cdot\mathbf{s}$ is the dot product of the orbital angular momentum. The calculations, while straightforward, are sufficiently tedious to require the use of a high-speed computer. All of the even parity states from −4.14 Mev up to 2.0 Mev are well described by the following set of parameters (Corman and Fowler, 1960):

for s states and s phase shifts,

$$V_0 = -50.3 \text{ Mev} ,$$
$$R = 3.34 \times 10^{-13} \text{ cm} ,$$
$$\delta = 0.5 \times 10^{-13} \text{ cm} ;$$

for d states,

$$V_0 = -47.0 ,$$
$$R = 3.34 \times 10^{-13} \text{ cm} ,$$
$$\delta = 0.5 \times 10^{-13} \text{ cm} ,$$
$$\gamma = 19.3 .$$

In Fig. 3 the insert shows a plot of the potential well calculated from the set of parameters tabulated above. The dashed curves are the s- and d-wave (even parity) phase shifts calculated with the Woods-Saxon potential. There is good agreement with the measured phase shifts (Fowler and Cohn, 1958), which are indicated by the data points.

The phenomenological potential discussed above not only describes the bound states and some of the virtual states arising from the interaction of a neutron with O^{16}, but it also forms the starting point for a more detailed quantum mechanical analysis of the nucleus O^{17}. For example, the wave functions given by the potential can be used in calculating the γ-ray emission probability between the first excited state of O^{17} and the ground state (Barton, Brink, and Delves, 1959). The wave functions also can form the basis of a calculation of the energy levels of nuclei above O^{17}, such as O^{18} and F^{18}. These wave functions correspond, in fact, to the hydrogen atom-like wave functions

which are so important in atomic spectroscopy. Most energy levels of nuclei, however, are not as simple as the single-particle levels discussed here. Indeed, the odd-parity levels of O^{17} as well as the higher energy levels are not of the single-particle character. As in the case of complicated atoms, nuclear levels in general show a great deal of configuration mixing. These nuclear levels have a considerably longer lifetime than that expected from single-particle resonances. Such long-lived nuclear states are called compound nucleus states.

The introduction of phenomenological potentials greatly improves the fit to the total neutron cross sections at higher energies, $14 < E < 100$ Mev, discussed at the beginning of this article (Fig. 1). The simple analysis described in connection with these cross sections assumes that nuclei are totally absorbing for high-energy neutrons. This, in fact, is not the case; there is an appreciable probability of the incident neutron passing through the nuclear matter. At the surface of the nucleus the neutron is refracted by the average potential arising from the interaction with all of the other nucleons in the nucleus. The effects of both this refraction and of the absorption of neutrons can be represented by a potential of the Woods-Saxon form described above, to which has been added a term to simulate absorption. This latter is accomplished by the introduction of an imaginary term to the potential. This imaginary part of the potential is often chosen with the same radial dependence as the real part of the potential. A better over-all fit to the experimental data is obtained, however, if the imaginary part of the potential is peaked at the surface of the nucleus, which corresponds to absorption taking place mostly at the nuclear surface. The parameters which describe this "optical" potential are simple functions of neutron energy and atomic weight (Bjorklund and Fernbach, 1958). The real part of this "optical" potential is very similar to that shown in Fig. 3; the depth, which is a function of neutron energy, is comparable in the two cases; the surface thicknesses determined by δ in Eq. (16) are similar; and the effective radius of the "optical" potential, the r_0 of Eq. (16), increases with atomic weight A as follows:

$$r_0 = 1.25 \times 10^{-13} A^{1/3} \text{ cm} .$$

With such simple phenomenological expressions, one is able to correlate very many neutron measurements and even predict neutron cross sections for the practical needs of reactor engineering where measurements are difficult, or impossible.

LITERATURE CITED

Ajzenberg-Selove, F. and T. Lauritsen. 1959. Energy levels of light nuclei, VI. *Nuclear Phys.* 11:1.

Barton, G., D. M. Brink, and L. M. Delves. 1959. Quadrupole enhancement in O^{17} and F^{17}. *Nuclear Phys.* 14:256.

Bjorklund, F. and S. Fernbach. 1959. Optical-model analyses of scattering of 4.1-, 7-, and 14-Mev neutrons by complex nuclei. *Phys. Rev.* 109:1295.

Blatt, J. M. and V. F. Weisskopf. 1952. *Theoretical Nuclear Physics.* Wiley, New York, p. 324.

Corman, E. G. and J. L. Fowler. 1960. Phenomenological nuclear potentials from neutron scattering from O^{16}. *Bull. Am. Phys. Soc.* 5:34.

Eisenbud, L. and E. P. Wigner. 1958. *Nuclear Structure.* Princeton University Press, Princeton, N.J., chap. 7.

Fowler, J. L. and H. O. Cohn. 1958. Oxygen differential neutron scattering and phenomenological nuclear potentials. *Phys. Rev.* 109:89.

Hughes, D. J. and R. B. Schwartz. 1958. *Neutron Cross Sections.* Brookhaven National Laboratory Document No. 325, Second Edition.

Marion, J. B. and J. L. Fowler (Editors). 1960–61. *Fast Neutron Physics.* Interscience, New York.

Revs. Modern Phys. 30:412–584. 1958. See papers on international congress on nuclear sizes and density distribution.

Sherr, R. 1945. Collision cross section for 25-Mev neutrons. *Phys. Rev.* 68:240.

Schiff, L. I. 1955. *Quantum Mechanics.* McGraw-Hill, New York, p. 92F.

Thomas, L. H. 1926. The motion of the spinning electron. *Nature* 117:514; Inglis, D. R. 1936. Spin orbit coupling in nuclei. *Phys. Rev.* 50:783.

Woods, R. D. and D. S. Saxon. 1954. Diffuse surface optical model for nucleon-nuclei scattering. *Phys. Rev.* 95:577.